Front. For. China 2009, 4(3): 297–303
DOI 10.1007/s11461-009-0039-x

RESEARCH ARTICLE

Bin FANG, Qingke ZHU, Wenhua LI, Wei QIN

Dynamic emulation of the effect from a single tree to lower solar radiation distribution

Abstract By modeling the condition of light climate, we studied the negative effect of shadows in a shelterbelt forest. Based on the calculation of the apparent trajectory of solar motion according to an ellipsoid crown projection model and a Monsi light transmission model, radiation values of 36 experimental sites were measured using a light quantum meter. Estimates of daily solar radiation distribution from measured values were obtained. We built a crown projection model and simulated the conditions of a light climate in the forest. The trajectory of the shadow motion is shaped like a butterfly arc. The situation of the outside is affected by tree height (H) and that of the inner arc by height below the branches. In an area of $1.0 \times H$ (toward the east and west of the tree) and $0.6 \times H$ (toward the north), transmittance was below 90%, which means that the effect of shadow hazards occurs in this area. As well, the effect was strong at the bottom of the tree. The area of shadow hazards in the east and west of the tree was large and small in the south. The projection area of the shelterbelt forest was largest along an east and west direction. A certain distance between crops and the shelterbelt should be maintained when the shelterbelt is in a north-south direction. Therefore, the effect of shadow hazard will decrease north of the tropic of cancer. Cutting out the lower branches from the trees of the existing shelterbelt in a suitable and timely manner can reduce the area of the shadows.

Keywords protection forest, *Populus tomentosa* Carr, variation in shadows, solar radiation distribution, dynamic emulation

Translated from *Journal of Northwest A&F University*, 2008, 36(6): 113–118 [译自: 西北农林科技大学学报]

Bin FANG, Qingke ZHU (✉), Wei QIN
School of Soil and Water Conservation, Beijing Forestry University, Beijing 100083, China
E-mail: xiangmb@bjfu.edu.cn

Wenhua LI
College of Forestry, Northwest A&F University, Yangling 712100, China

1 Introduction

Solar radiation is a motive power for green plants to transfer light energy to biotic energy through photosynthesis. The study on the effect of light on forests began in the 1950s. Monsi and Saeki (1953) described the relationship between the attenuation of total radiation within plants and leaf area index using the Bouguer formula and presented the well-known Monsi model. After that, geometric and statistical models became the focus of research in illumination and simulation models. Kastrov (1955), Szwarzbaum (1976), Jahake (1965), and Thornley et al. (1989) simulated single plants with approximate geometries, establishing geometric models for cylinders, spheres, cones, and ellipsoids, respectively. The most typical model is the illumination model built by Norman and Wells (1983) in 1983. Since the 1960s, much research progress in this field has been made in China. Wang (1961) and Hong (1963) studied light intensity distribution in plant communities. He and Liu (1980) measured light reflection, transmission, and absorption rates, indicating the changes in total solar radiation in three kinds of conifers. Cui and Zhu (1981) made a theoretical analysis of the crown structure and light distribution of protective forests. Liu et al. (1990) and Wang (1991) explored the light environment of agroforestry systems.

Forests that protect farmlands can serve as a green ecological barrier for crop farming, provide timber, and play an important role in establishing a new socialist countryside and beautifying rural environments. Light is referred to as a light climate in the growth of plants. In agroforestry ecosystems of the Loess Plateau, light is an important factor in the field of ecology, along with moisture, nutrients, and other environmental factors that affect and determine the growth of plants (Lu et al., 1999). Because the forest canopy changes the light conditions, protection forests in agriculture have a great impact on the growth of farm crops in areas where farming and forestry intersect. Therefore, studying solar radiation transmission within the canopy and building an illumination model for forests to describe quantitatively the solar radiation

distribution under forest cover and determine the light climate of crops in the forests are of importance when estimating the reduction of threats from the shade of farm shelterbelts, the increase in crop productivity, and a suitable establishment of a protective agricultural forest system. *Populus tomentosa* Carr., a common tree species in protection forests in the Loess Plateau, is used as a study objective. Given the characteristic structural parameters of individual crowns and the equation of the trajectory of the sun in the study area, a projection model of a single crown of *P. tomentosa* Carr. is established, and the space-time distribution of the light climate under forests is simulated. We have analyzed the negative impact for crops under protection forests to provide a theoretical basis for building protective agricultural forests and configuring an agroforestry ecosystem in the Loess Plateau.

2 Study site

The study area is located in Jixian County, Shanxi Province (36.29°N, 110.63°E), at an elevation of 920 m. As a typical residual area in the Loess Plateau in this gully and beam-hilly region, it has a temperate continental climate with an average annual precipitation of 580 mm, an average annual temperature of 11°C, an average number of accumulated sunshine of 2563.8 h, and an average annual frost-free period of 127 d. Its soil is a cinnamonic soil, with loess parent material.

3 Methods

At first instance, one 10-year-old *P. tomentosa* tree from three rows of an agricultural protective forest belt was selected as study objective, with its structural crown parameters such as the clear length, crown length, crown width, leaf azimuth, leaf lean angle, angle between branch, and stem to be measured. According to these parameters, the crown projection was simulated with an ellipsoid model and the change of the solar altitude. Next, the motion trail of shade varying with solar altitude was drawn using a crown projection model and the Monsi model, expressing the mechanism of light transmission within the crown. A rectangular coordinate system with an origin based on the central position of the tree's bottom was established. Subsequently, for every two hours, the radiation value of 36 experimental sites under the tree was measured by a quantometer, and their point coordinates were recorded. The number of points with 10%, 30%, 45%, 60%, 75%, and 90% transmittance were 4, 4, 6, 6, 8, and 8, respectively. If the total radiation of the open ground and shaded areas under the forest is R_o and R_i, respectively, the transmittance under forest is $R_i/R_o \times 100\%$. In the end, a distribution map of light intensity, in percentages, was made using the transmittance of every test point calculated according to its light intensity accumulation for analyzing the changing characteristics of the light climate under the tree.

4 Results and analysis

By and large, the formation of microclimates is mainly affected by solar altitude, hour angle, and terrain (He, 1986). Because of their direct impact on the number of sunlight hours and radiant intensity, the relief form, the direction of the mountain range, slope grade, and slope position can metabolize airflow and change the heat received per unit area of different slope positions (Fu, 1998; Zeng et al., 2005; Liu et al., 2007). On a microscale level, studies on the light climate focus on analyzing and simulating the three-dimensional space structure of the vegetation. The surface vegetation system is a multilayer spatial structure composed of moss, lichens, herbage, shrubs, and trees. In the course of passing through the crown, sunlight reflects, absorbs and transmits repeatedly, and forms new distributions of radiation intensity.

4.1 Computation of apparent solar motion path

Sunlight is an incident light source in the formation of forest shadows. The variation in the apparent solar motion path will give rise to changes in the incident angle. Therefore, calculating the solar altitude (α) and the hour angle (ω) is the key to determine the apparent solar motion path. Their calculation formulas are as follows:

$$\sin\alpha = \sin\varphi\sin\delta + \cos\varphi\cos\delta\cos\omega \quad (1)$$

$$\delta = (e-f) \times (g+i+k) + f \quad (2)$$

$$\omega = (\text{apparent solar time} - 12) \times 15 \quad (3)$$

$$\text{apparent solar time} = \text{teilchron} + \text{time difference} \quad (4)$$

$$\text{teilchron} = \text{Beijing time} + (\text{longitude} - 120) \times 4 \quad (5)$$

where α stands for the elevation angle of the sun, that is, the angle included between the direction of incidence sunlight and the horizon line at the observation point; φ is the geographic latitude; δ is the declination, that is, the angle distance measured at any point on the earth's surface between the sun-earth line and the equatorial plane in the equatorial coordinate system whose basic plane is the equator; e is the morrow declination; f is the day declination; g is the annual revised value; i is the revised longitudinal value; and k is the revised time value.

When the sun rotates to the north, δ is positive and negative when rotating to the south of the equatorial plane. The daily variations of declination can be obtained from common tables of solar radiation observations. However,

since common tables are calculated based on zero longitude and zero time in 1925, three revisions (i.e., an annual revision, a longitudinal revision, and a time revision) have to be made when calculating a value for δ at any time and location. These revised values can be obtained from revision tables calibrated by dates.

One apparent solar time is the time interval that the sun passes through the meridian twice during the continuous rotation of the earth. The apparent solar time is divided into 24 equal portions, each portion being an hour of solar time and equal to 15°. The angle turned from apparent solar time is called the hour angle (ω) whose zero degree is noon (12: 00). Clockwise direction is positive, and counterclockwise is negative.

In China, east 120° longitude serves as standard time, called Beijing time. It is needed to convert Beijing time to local time, plus the time difference to obtain the hour angle.

The geographic coordinates of the study area are north latitude 36.29° and east longitude 110.63°. The calculated results of solar elevation at noon are listed in Table 1. Then, on the basis of local sunrise and sunset times from the meteorological common table (Table 2), the apparent solar motion path is presented (Fig. 1).

Figure 1 shows four special apparent solar motion paths in Jixian County. It should be noted that the highest solar elevation is at noon (12:00) of any day, and the solar elevation in summer is higher than that in winter during a particular year. The highest number of sunshine hour is during the summer solstice (22 June), when the days are long, and the nights are short. At the winter solstice (22 December), this is reversed. At the vernal equinox (21 March) and autumnal equinox (21 September), the length of both day and night is 12 h.

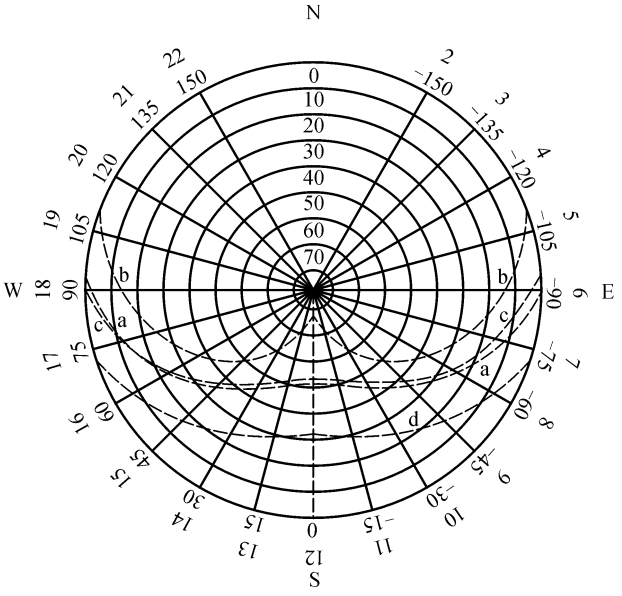

Fig. 1 Illustration of apparent trajectory of solar motion in experimental area
Note: a: vernal equinox (21 Mar.); b: summer solstice (22 Jun.); c: autumnal equinox (21 Sept.); d: winter solstice (22 Dec.).

4.2 Simulation model of solar radiation

The interaction in the soil between the protection forest and crops is mainly demonstrated as a competition for water and nutrients. Their interactions on the ground are largely presented as a negative impact of forest on crops (Zhu and Zhu, 2003). The light climate of a species in a forest always changes in the time and radiant intensity from the hazard of

Table 1 Example of solar altitude in experimental area

	ω/°				δ/°					sinα	α/°
	teilchron	time difference /min	apparent solar time	hour angle /°	day declination	morrow declination	declination difference	revised values	declination /°		
vernal equinox (21 Mar.)	11:23	−8	11:15	−11.5	−0.1	0.3	0.4	0.2	−0.02	0.790	52.15
	12:08		12:00	0						0.806	53.69
summer solstice (22 Jun.)	12:23	−1	11:22	−9.5	23.4	23.4	0	0.2	23.4	0.965	74.72
	12:01		12:00	0						0.975	77.11
autumnal equinox (21 Sept.)	13:23	7	11:30	−7.5	1	0.6	−0.4	0.2	0.92	0.809	53.95
	11:53		12:00	0						0.815	54.63
winter solstice (22 Dec.)	14:23	2	11:25	−8.75	−23.4	−23.4	0	0.2	−23.4	0.496	29.74
	11:58		12:00	0						0.505	30.31

Note: The revised values are the sum of the annual revised value, the longitudinal revised value, and the temporal revised value.

Table 2 Example of sunrise and sunset time-table in experimental area

time	vernal equinox (21 Mar.)	summer solstice (22 Jun.)	autumnal equinox (21 Sept.)	winter solstice (22 Dec.)
sunrise	06:03	04:46	05:47	07:07
sundown	18:12	19:17	17:59	16:49

shadows under tall trees. Crown projection models express these changes intuitively.

4.2.1 Simulation model of crown projection

Canopy structure refers to the amount and spatial arrangement of plant organs above the ground and includes shape, size, location, growth position, angle and dynamic changes over time and space of leaves, stems, branches, flowers, and fruits. All of these form the basis in deciding the characteristic differences of crown radiation in each direction (Zhao et al., 2006). Studies about plant crown structures are the basis for simulating plant-environment interactions and plant community productivity. *P. tomentosa*, a kind of woody plant, has a wide oval crown, terminal buds, and monopodial branches. This species has both long and short branches. Belonging to an open mode, its lateral branches have more withies, are phototropic, and grow continuously outward and sprout new branches leading to an area expansion from which the crown receives its sunlight. The separated angle of lateral branches always varies between 60° and 90°. *P. tomentosa* is a species of simple alternate leaves. The leaf area of short branches is slightly larger than that of long branches. The leaf shape of long branches is oval or triangular, 10–15 cm long and 7–13 cm wide (Ren, 1997). The angle of the leaf with respect to the level (known as the leaf dip angle) and the leaf with respect to the north (known as the leaf azimuth angle) form a continuous distribution and a random distribution, respectively. Because the leaf angle of *P. tomentosa* corresponds to an ellipsoid surface distribution, an ellipsoid body distribution model was chosen to simulate its crown (Fig. 2).

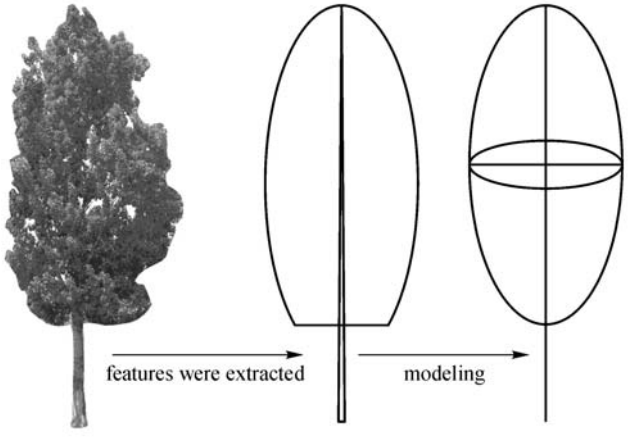

Fig. 2 Illustration of tree crown of *P. tomentosa* Carr.

Figure 3 shows the space coordinate system, where the center of the crown ellipsoid is the origin. In this coordinate system, an arbitrary point on the crown can be presented by $(X, Y, Z)_t$. When moving the origin of the coordinate system to the ground, the coordinates of the arbitrary point will change to $(X', Y', Z')_t$. This can be expressed as follows:

$$\begin{cases} X' = X \\ Y' = Y \\ Z' = Z + \dfrac{h+H}{2} \end{cases} \tag{6}$$

For example, in the previous coordinate system, the coordinates of the origin are $(X, Y, Z) = (0, 0, 0)$. In the new coordinate system, its coordinate will become $(X', Y', Z') = \left(0,\ 0,\ \dfrac{H+h}{2}\right)$.

When substituting the solar incidence direction vector $v = \dfrac{1}{\sqrt{1+\mathrm{tg}^2\omega}}(\cos\alpha, \sin\alpha, \mathrm{tg}\omega)^t$ into the above formula (6), given the coordinate transformation formula, the crown projection model can be expressed as:

$$\begin{cases} X'' = X - \left[Z + \dfrac{h+H}{2}\right]\cos\alpha \cdot \mathrm{ctg}\omega \\ Y'' = Y - \left[Z + \dfrac{h+H}{2}\right]\sin\alpha \cdot \mathrm{ctg}\omega \end{cases} \tag{7}$$

where $X \subseteq [-a, +a]$, $Y \subseteq [-b, +b]$, $Z \subseteq [h, H]$, a and b are the directly measured crown length and crown width, respectively; H stands for tree height, h is the clear length, α is the solar altitude, and ω is the hour angle (Lu et al., 1999).

In accordance with Eq. (7), the shadow position, area, and other relevant indices of any point on the crown projecting to the ground can be calculated.

Figure 3 also shows that solar altitude has an impact on

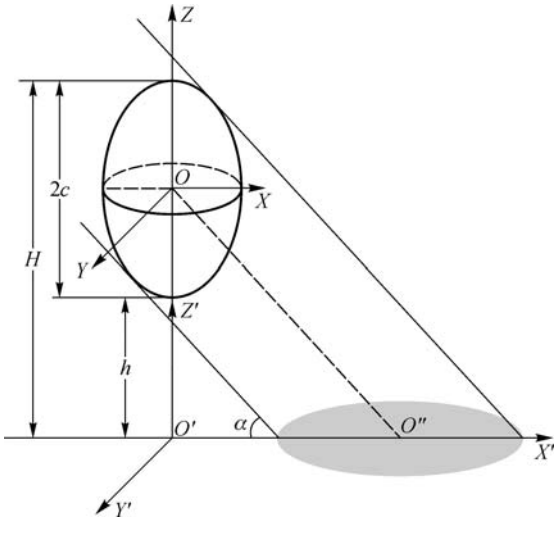

Fig. 3 Emulation scheme of tree crown projection of *P. tomentosa* Carr.

the shape and size of crown projection ($2c$ is the height of the crown). The larger the solar elevations, the nearer the crown projection to the position of the tree; the smaller the crown projection area, the longer the distance of sunlight through the crown. The larger the tree height, the further the crown projection from the position of the tree; the longer the semimajor axis of the projection ellipse and the bigger the shaded crown area, the smaller the clear length. As well, the nearer the crown projection to the position of the tree, the shorter the semimajor axis of the projection ellipse and the bigger the shaded crown area. For this reason, when building a protective forest, it can reduce the area of shade, which negatively impacts crops by proper trimming of the lower branches and by increasing its clear length.

4.2.2 Transmission of solar radiation in the crown

A proportional relationship exists between the attenuation of solar radiation through leaves and luminosity of the plant crown, radiant intensity, and the number of leaf layers through which radiation passes. According to the Monsi model, by carrying out integration, the following result is obtained:

$$I = I_0 \mathrm{e}^{-(r+d)} L_m \cdot z \tag{8}$$

where I stands for emergent light intensity; I_0 stands for incident light intensity; r and d are the reflection and absorption coefficients, respectively; L_m is the density of leaf area; and z is the transmission distance of incident light in tree leaves.

Equation 8 shows that the larger the density of leaf area, the longer the transmission distance of the incident light and the greater the extinction of light by the crown. If the change in leaf shape in its growth process is ignored, then solar elevation is the major factor affecting the incidence of leaf shade. Given the measurements of reflectivity and transmittancy of a simple leaf (Table 3), these indicate that both reflectivity and transmittancy of simple leaves have an inverse proportional relationship with solar elevation. Reflectivity and tansmittance are lowest at noon, when solar elevation reaches its maximum.

4.3 Dynamic emulation of radiation transfer

4.3.1 Shadow motion path

By using the crown projection model, the motion path of shadows at four special solar terms (vernal equinox, summer solstice, autumnal equinox, and winter solstice) for one year was calculated (Fig. 4).

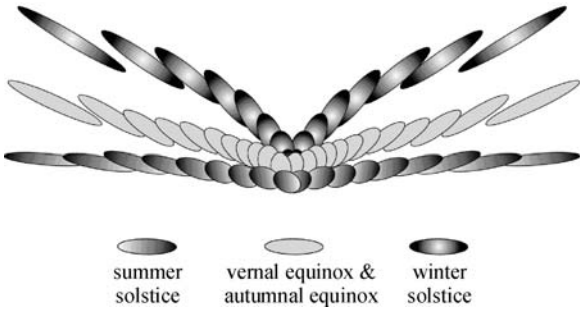

Fig. 4 Illustration of the track of annual moves of the shadow of an isolated tree

According to Fig. 4, the projection position of a single tree varies with solar elevation over a one-year period, making an arc in the form of a butterfly, where the projection positions in the summer and winter solstices are located in the north and south end points of the arc, respectively. The arc moves from the position of the tree to the north every day in a sequence of summer solstice-autumnal equinox-winter solstice and to the south daily in a reverse pattern after the winter solstice. The projection belts of forenoon and afternoon are symmetrical and centered at noon. The angle between them decreases daily in a sequence of summer solstice-autumnal equinox-winter solstice and increases every day in a reverse sequence after the winter solstice. The shadows at sunrise and sunset can be neglected for they are indistinct. In our study area, the shadow of a single tree varies between ($\pm$8a, 2b) in one year (where a stands for crown length and b for crown width).

4.3.2 Light intensity distribution in the shade

It is not enough to express the characteristics of a photosynthetic environment and the negative effect of forests on farmland, only by knowing the motion path of the shadow and its area. The time of shading and intensity also need to be taken in consideration to investigate the light climate in forests and express the change of light climate. In an area with over 90% transmittance, no clear discrepancy was found in light intensity on land without forests (Lu et al., 1999). Therefore, on the basis of the measurement data from our 36 test points, a distribution map of solar radiation in forests, where the origin was

Table 3 Daily variation of reflectivity and transmittance from a single leaf of *Populus tomentosa* Carr. (Aug. 21, 2007)

time	09:00	10:00	11:00	12:00	13:00	14:00	15:00	16:00
reflectivity/%	14.9	12.8	11.2	9.7	11.5	13	14.7	16.1
transmittance/%	10.4	8.2	6.5	5.4	6.7	8.4	10.3	11.1

based on the position of the tree and transmittance of less than 90%, was made (Fig. 5).

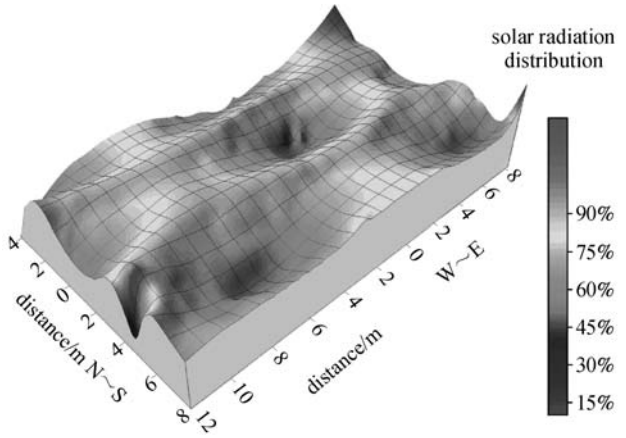

Fig. 5 Illustration of solar radiation distribution in a forest

Figure 5 is the distribution map of solar radiation under the 10-year-old *P. tomentosa* tree with a crown width of 3.0 m, a crown length of 5.9 m, and a tree height of 8.7 m during its time of bloom (August). Figure 5 shows that, centering on the bottom of the tree, an area with a transmittance of less than 90% falls in a range of $1.0 \times H$ to the east and west of the tree and of $0.6 \times H$ to the north of the tree. In the east and west of the tree, the shadow area was large, but the gradient of solar variation was small. To the south and north, they were just the reverse. The negative impact on crops is stronger at the bottom of the tree; the transmittance and solar radiation are small in this area, in contrast to being further away from the tree. The negative impact on crops is strong near the position of the tree where transmittance and solar radiation are small. In the range further away from the tree, they are just the reverse. Because our study area was located north of the tropic of cancer, the shady south area of the tree was smaller than all the areas at the other sides.

5 Conclusions

According to the simulation of the path of variation in the shadow of a tree and the light intensity distribution under this tree in an experimental area, we arrive at the following conclusions.

The crown projection model used in our investigation was the best model to carry out dynamic simulation of crown projections in our experimental area.

As shown in the crown projection simulation, solar elevation impacts crown projections. When light intensity is constant, the larger the solar elevation, the longer the distance of sunlight through the crown, the greater the extinction, and the smaller the crown projected area.

The emulation of shadow under the tree indicated that the component and form of the crown affect the shadow area under the tree. The path of variation of the shadow forms a limited butterfly arc and moves cyclically in the following sequence: vernal equinox-summer solstice-autumnal equinox-winter solstice-vernal equinox. Furthermore, conditions outside the arc are affected by the tree height, and those inside the arc area are affected by the height below the branches.

The transmission emulation under the tree shows that transmittance is below 90%, ranging from $1.0 \times H$ in the east and west to $0.6 \times H$ in the north around the position of the ten-year-old *P. tomentosa* tree in our study area. As well, the negative impact on crops is strong near the bottom of the forest shelterbelt. The negative-effect area of the shadow around the tree decreases in the following sequence: in the east and west > in the north > in the south.

The characteristics of ecological factors in agroforestry systems are the basis for investigating the interaction between protection forests and crops. Our study has emulated the crown projection and light intensity distribution in a forest, which provides a useful supplement for research on airflow features in agroforestry systems (Fan et al., 2002) and in the characteristics of change of soil moisture and nutrients (Huang, 1985).

The shading function of protective forests not only affects the intensity of solar radiation but also changes the quality of light in forests. The change of light quality has a direct bearing on the growth of plant organs and the vitality of undergrowth (Sylvie, 1999). Therefore, research on light climate requires further studies on the effect of forestry on the quality of light.

Acknowledgements This study was supported by the National Key Technologies Research and Development Program in the eleventh Five year Plan (No. 2006BAD03A03) and the Graduate Fund Projects of Beijing Forestry University (No. 06JJ024).

References

Cui Q W, Zhu J W (1981). Forest canopy structure and optical radiation distribution — Theory of optical transmission and reflection. Acta Geogr Sin, 36(2): 196–208 (in Chinese)

Fan Z P, Zeng D H, Zhu J J, Sha J G, Jiang F J (2002). Advance in characteristics of ecological effects of farmland shelterbelts. J Soil Water Cons, 16(4): 130–133 (in Chinese)

Fu B P (1998). The difference change of income and expenses ingredients of solar radiation over different terrains. Chin J Atmos Sci, 22(3): 178–190 (in Chinese)

He Q T (1986). Aerography. Beijing: China Forestry Publishing House (in Chinese)

He Q T, Liu Z C (1980). Thermal balance of forest. Sci Silv Sin, 16(1): 24–33 (in Chinese)

Hong Q F (1963). Micro micromate of *Pinus massoniana* young stand. Sci Silv Sin, 8(4): 275–289 (in Chinese)

Huang Y L (1985). The activity and variation of soil moisture and

nutrients under *Paulownia*-crops interplanting. Sci Silv Sin, 21(3): 292–297 (in Chinese)

Jahake L S (1965). Influence of photosynthetic crown structure on potential productivity of vegetation based primarily on mathematical models. Ecology, 46: 319–326

Kastrov U G (1955). On the diurnal course of the albedo of the Earth's surface Trans. Aerol Obs, 14: 12–22

Liu N Z, Xiong Q X (1990). Simulating of solar radiation on intercropping farmland of crop plant and *Paulownia*. Paulownia Agro-For, 2: 18–29 (in Chinese)

Liu S, Qiu X F, Wang X Y (2007). Distributed modeling of diffuse solar radiation over rugged terrains of China. J Nanjing Inst Meteorol, 30 (3): 371–376 (in Chinese)

Lu Q, Zhao T S, Shi Y Q (1999). Theory and Methodology on Simulating Agroforestry System. Beijing: China Environment Science Press (in Chinese)

Monsi M, Saeki T (1953). Uber den Lichtfaktor in den pflanzengesell schaften und seine bedeutung fur die Stoffproduktion. Jap J Bot, 14: 22–52

Norman J M, Wells J M (1983). Radiative transfer in an array of canopies. Agric J, 75: 481–488

Ren X W (1997). Dendrology. Beijing: China Forestry Publishing House (in Chinese)

Sylvie P (1999). Root response to above-ground light quality. Plant Physiol, 141: 67–77

Szwarzbaum I (1976). A montecarlo model for the radiation field in plant canopies. Agric Meteorol, 17: 333–352

Thornley J H M (1989). A model of nitrogen flows in grassland. Plant Cell Environ, 12: 863–886

Wang H J (1991). Solar energy distribution in agroforestry ecosystem. Chin J Ecol, 10(1): 27–32 (in Chinese)

Wang T D (1961). Modeling of optical radiation distribution and photosynthesis from paddy rice group. In: Yin H Z, ed. Proceedings of Paddy and Wheat. Shanghai: Shanghai Science and Technology Press, 33–50 (in Chinese).

Zeng Y, Qiu X F, Liu S M (2005). Distributed modeling of extraterrestrial solar radiation over rugged terrains. Chin J Sin, 48 (5): 1028–1033 (in Chinese)

Zhao F, Gu H F, Liu Q, Yu T, Chen L F, Gao H L (2006). Modeling of 3D canopy's radiation transfer in the VNIR and TIR domains. J Rem Sens, 10(5): 670–675 (in Chinese)

Zhu Q K, Zhu J Z (2003). The Continuable Technology of Returning the Gain Plots to Forest of the Loess Plateau. Beijing: China Forestry Publishing House (in Chinese)